Proc. Symposium IEEE Benelux Chapter on Communications and Vehicular Technology, 2003 (SCVT2003), Eindhoven, The Netherlands, Nov. 2003, paper 08.

Analysis of the Influence of Phase Noise in MIMO OFDM based WLAN systems

Tim C.W. Schenk*† and Paul Mattheijssen‡
*Agere Systems, PO Box 755, 3430 AT Nieuwegein, The Netherlands
†Eindhoven University of Technology, PO Box 513, 5600 MB Eindhoven, The Netherlands, T.C.W.Schenk@tue.nl
‡ Philips Research Laboratories, Prof. Holstlaan 4, 5656 AA Eindhoven, The Netherlands, paul.mattheijssen@philips.com

***Abstract*— The influence of phase noise (PN) on the performance of a multiple-input multiple-output (MIMO) orthogonal frequency division multiplexing (OFDM) based communication system is analyzed. A PN power weighting function is derived which indicates the influence of the different subcarriers and the shape of the PN spectrum. For compensation of the common phase error (CPE), the maximum likelihood estimation of the CPE is shown to be equal to a determinant criterion optimization. For practical implementation an estimator with reduced complexity is found, for which an upper bound on the error is found. Using this bound the resulting PN spectrum after compensation can be found, which enables the derivation of the effect of the residual PN. The performance of the compensation scheme in an additive white Gaussian noise (AWGN) environment and resulting bit-error-rate (BER) are shown using results from simulations.**

I. Introduction

Orthogonal frequency division multiplexing (OFDM) has been adopted by the wireless local-area-network (WLAN) standards IEEE 802.11a [1] and g [2]. The main advantages of OFDM are its high spectral efficiency and ability to deal with frequency selective fading and narrowband interference. The spectral efficiency of OFDM systems can be further increased by the addition of multiple antenna techniques, also known as multiple-input multiple-output (MIMO) techniques. The indoor deployment of WLANs makes MIMO OFDM a strong candidate for high throughput extensions of current WLAN standards [3], since the throughput enhancement of MIMO is especially high in richly-scattered scenarios of which indoor environments are typical examples.

The performance of single-input single-output (SISO) OFDM systems is jeopardized by radio impairments like phase noise (PN). PN occurs when the power spectral density (PSD) of the local oscillator (LO) does not resemble a delta function, which is the case for all practical oscillators. Various papers show the influence of PN on the performance of a SISO OFDM system [4–6]. Several compensation schemes for PN in OFDM systems have been proposed, among others in [6–8], using either pilot data or decision feedback. To the best of the authors' knowledge no study concerning the influence of, or compensation scheme for PN in a MIMO OFDM system has been published.

Therefore, this paper analyzes the influence of PN on the performance of a multiple antenna OFDM system. The influence is derived analytically and shown to affect the MIMO OFDM signal. It is shown that PN causes, similarly to the SISO case, a common phase error (CPE) and an inter-carrier-interference (ICI) term. A weighting function for the PN power shows the influence of the different frequencies components in the PN spectrum. For compensation of the CPE, we show that the maximum likelihood (ML) estimation of the CPE equals optimization of a determinant criterion. For practical implementation a reduced-complexity estimation and compensation approach is derived. A lower bound on the performance of this estimator is derived, analytically. We show that next to the relative frequency, the error dependents on the signal-to-noise-ratio (SNR) and number of antennas and pilots. Using this error bound, the suppression by the compensation can be found. Furthermore, we compare the analytically derived performance measure for the compensation with that from Monte Carlo simulations. Also the bit-error-rate (BER) of MIMO OFDM systems experiencing PN is shown, with and without application of the proposed compensation scheme.

The organization of the paper is as follows. In Section II the MIMO OFDM signal model is defined and the influence of PN is shown. Two estimation and compensation schemes are introduced and evaluated in Section III. Section IV elaborates on the impact of PN before and after CPE correction. Section V then numerically evaluates the performance of the compensation scheme and the influence of PN on the BER performance using Monte Carlo simulations. Finally, conclusions are drawn in Section VI.

II. System model for MIMO OFDM including RF imperfection

A. MIMO OFDM signal model

Suppose that a MIMO OFDM system consists of N_t transmit (TX) and N_r receive (RX) antennas, denoted as a $N_t \times N_r$ system. Let us define the a-th MIMO OFDM vector to be transmitted as $\hat{\mathbf{s}}(a) = \left(\mathbf{s}^T(0,a), \mathbf{s}^T(1,a), \ldots, \mathbf{s}^T(N_c-1,a)\right)^T$, where $\mathbf{s}(n,a)$ denotes the $N_t \times 1$ frequency domain MIMO transmit vector for the n-th subcarrier and N_c represents the number of subcarriers. This vector is transformed to the time domain using the inverse discrete Fourier transform (IDFT)

$$\hat{\mathbf{u}}(a) = \left(\mathbf{F}^{-1} \otimes \mathbf{I}_{N_t}\right) \hat{\mathbf{s}}(a) \ , \qquad (1)$$

where $\otimes$ denotes the Kronecker Product, $\mathbf{F}$ is the $N_c \times N_c$ Fourier matrix, of which the (i,k)-th element equals $\exp(-j2\pi\frac{ik}{N_c})$, and $\mathbf{I}_N$ represents the $N \times N$ dimensional

identity matrix. A cyclic prefix (CP) is added to the signal $\hat{\mathbf{u}}(a)$ by multiplication with matrix $\mathbf{\Theta}$, which adds the last $N_t N_g$ elements of $\hat{\mathbf{u}}(a)$ on top of $\hat{\mathbf{u}}(a)$. Here, N_g denotes the CP length for one TX antenna. We assume (at least for this section and in the PN analysis of Section III) that N_g is higher than the channel impulse response (CIR) length, avoiding inter-symbol-interference (ISI). It is assumed that the average total TX power P_t is equally divided among the TX antennas.

The signal is then upconverted to radio frequency (RF) and transmitted through the quasi-static multipath channel, represented by matrix $\mathbf{C}$. The average channel attenuation and delay are assumed to be unity and zero, respectively.

At the RX side the signal is down converted to baseband with the RF LO, where the a-th received $N_{\text{tot}} N_r \times 1$ time domain symbol is given by $\hat{\mathbf{r}}(a) = \left(\mathbf{r}^T(aN_{\text{tot}}), \ldots, \mathbf{r}^T(aN_{\text{tot}} + N_{\text{tot}} - 1)\right)^T$, where $\mathbf{r}(m)$ denotes the $N_r \times 1$ receive vector at sample instant m and $N_{\text{tot}} = N_g + N_c$ is the total symbol length. The CP is removed (*Rmv CP* in Fig. 1) by multiplication with $\mathbf{\Theta}^{-1}$, which removes the first $N_r N_g$ elements of $\hat{\mathbf{r}}(a)$. The received signal $\hat{\mathbf{y}}$ is converted to the frequency domain using the discrete Fourier transform (DFT), which yields

$$\begin{aligned}\hat{\mathbf{x}}(a) &= (\mathbf{F} \otimes \mathbf{I}_{N_r})\hat{\mathbf{y}}(a) = (\mathbf{F} \otimes \mathbf{I}_{N_r})\mathbf{\Theta}^{-1}\hat{\mathbf{r}}(a) \\ &= (\mathbf{F} \otimes \mathbf{I}_{N_r})\mathbf{\Theta}^{-1}(\mathbf{C}\mathbf{\Theta}(\mathbf{F}^{-1} \otimes \mathbf{I}_{N_t})\hat{\mathbf{s}}(a) + \hat{\mathbf{v}}(a)) \\ &= \hat{\mathbf{H}}\hat{\mathbf{s}}(a) + \hat{\mathbf{n}}(a) \ , \end{aligned} \tag{2}$$

where $\mathbf{\Theta}^{-1}\mathbf{C}\mathbf{\Theta}$ is a *block circulant matrix* and $\mathbf{C}$ denotes the time domain MIMO channel matrix. The matrix $\mathbf{\Theta}^{-1}\mathbf{C}\mathbf{\Theta}$ can be diagonalized by the IDFT and DFT operation yielding the $N_c N_r \times N_c N_t$ block diagonal matrix $\hat{\mathbf{H}}$, which represents the frequency domain version of the channel matrix $\mathbf{C}$. The n-th $N_r \times N_t$ block diagonal element is $\mathbf{H}(n)$, the MIMO channel for the n-th subcarrier. The $N_r N_c \times 1$ vector $\hat{\mathbf{n}}(a)$ represents the frequency-domain noise, with i.i.d. zero-mean, complex Gaussian elements with a variance of σ_n^2 and $\hat{\mathbf{v}}(a)$ denotes its time-domain equivalent. It is clear from (2) that the carriers are orthogonal.

The system described above is depicted schematically in Fig. 1, where $\mathbf{E}_{\text{TX}}$, $\mathbf{E}_{\text{RX}}$ and *PN Comp* are added to model the influence of both PN and its compensation, as will be explained in Section II-B.

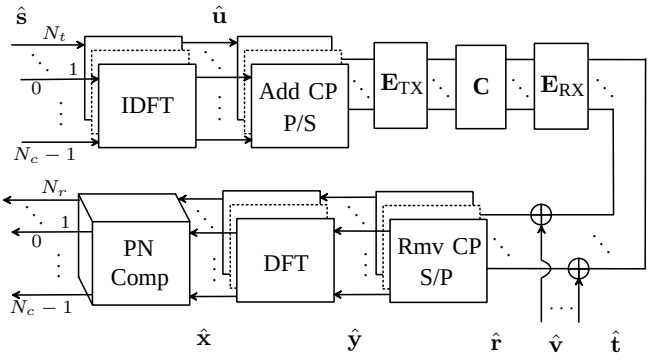

Fig. 1. MIMO OFDM system model with Phase Noise compensation.

B. Influence of Phase Noise

To introduce the influence of the radio impairment phase noise (PN) in the baseband signal model, we multiply the time domain signal at the transmitter and receiver with $\mathbf{E}_{\text{TX}}(a)$ and $\mathbf{E}_{\text{RX}}(a)$, respectively. In the following we leave out the symbol index a to increase the readability. The received signal after the DFT can be written as

$$\begin{aligned}\hat{\mathbf{x}} &= (\mathbf{F} \otimes \mathbf{I}_{N_r})\mathbf{\Theta}^{-1}\mathbf{E}_{\text{RX}}(\mathbf{C}\mathbf{E}_{\text{TX}}\mathbf{\Theta}(\mathbf{F}^{-1} \otimes \mathbf{I}_{N_t})\hat{\mathbf{s}} + \hat{\mathbf{v}}) \\ &= \mathbf{G}_{\text{RX}}\hat{\mathbf{H}}\mathbf{G}_{\text{TX}}\hat{\mathbf{s}} + \hat{\mathbf{n}} \ , \end{aligned} \tag{3}$$

where $\mathbf{E}_k = \text{diag}(e_0, e_1, \ldots, e_{N_{\text{tot}}-1}) \otimes \mathbf{I}_{N_l}$ denotes the phase distortion, with $e_m = \exp(j\theta_k(a,m))$, $k \in \{\text{RX}, \text{TX}\}$ and $N_l \in \{N_r, N_t\}$. Furthermore, $\theta_k(a,m) = \theta_k(aN_{\text{tot}} + m)$ is a real sampled random variable and represents the PN process. A typical distribution of this process is given in Section IV, but no assumption about it is made here. From (3) it is clear that $\mathbf{\Theta}^{-1}\mathbf{E}_{\text{RX}}\mathbf{C}\mathbf{E}_{\text{TX}}\mathbf{\Theta}$ is no longer block circulant and can thus not be diagonalized by the DFT and IDFT operations. This means inter-carrier-interference (ICI) will occur, which is modelled by the $N_c N_t \times N_c N_t$ matrix $\mathbf{G}_{\text{TX}}$ and $N_c N_r \times N_c N_r$ matrix $\mathbf{G}_{\text{RX}}$.

We now assume for further analysis that the TX does not experience PN, thus $\mathbf{E}_{\text{TX}} = \mathbf{I}_{N_{\text{tot}} N_t}$. The received signal is then given by $\hat{\mathbf{x}} = \mathbf{G}_{\text{RX}}\hat{\mathbf{H}}\hat{\mathbf{s}} + \hat{\mathbf{n}}$, where $\mathbf{G}_{\text{RX}}$ is given by

$$\begin{aligned}\mathbf{G}_{\text{RX}} &= (\mathbf{F} \otimes \mathbf{I}_{N_r})\mathbf{\Theta}^{-1}\mathbf{E}_{\text{RX}}\mathbf{\Theta}(\mathbf{F}^{-1} \otimes \mathbf{I}_{N_r}) \\ &= \begin{pmatrix} g_0 & g_{-1} & \cdots & g_{-(N_c-1)} \\ g_1 & g_0 & \cdots & g_{-(N_c-2)} \\ \vdots & \vdots & \ddots & \vdots \\ g_{N_c-1} & g_{N_c-2} & \cdots & g_0 \end{pmatrix} \otimes \mathbf{I}_{N_r} \ , \end{aligned} \tag{4}$$

and $g_q = \frac{1}{N_c} \sum_{n=0}^{N_c-1} \exp(j\theta(a, n + N_g)) \exp(-j2\pi qn/N_c)$. Since only RX PN is regarded the PN θ_{RX} has been replaced by θ. Note that the elements on the diagonal of $\mathbf{G}_{\text{RX}}$ result into a common phase error (CPE) and the other elements contribute to the ICI.

When the amplitude of the phase noise is small, we can use the first order approximation $\exp(j\theta(a,m)) \approx 1 + j\theta(a,m)$. Thus $\mathbf{E}_{\text{RX}} \approx \mathbf{I}_{N_{\text{tot}} N_r} + \mathbf{E}_1$, where $\mathbf{E}_1 = \text{diag}(\tilde{e}_0, \tilde{e}_1, \ldots, \tilde{e}_{N_{\text{tot}}-1}) \otimes \mathbf{I}_{N_r}$ and $\tilde{e}_m = j\theta(a,m)$. The received signal (3) can now be written as

$$\hat{\mathbf{x}} = \hat{\mathbf{H}}\hat{\mathbf{s}} + \tilde{\mathbf{G}}\hat{\mathbf{H}}\hat{\mathbf{s}} + \hat{\mathbf{n}} \ , \tag{5}$$

where the $N_c N_r \times N_c N_r$ matrix $\tilde{\mathbf{G}}$ denotes the influence of the PN on the received frequency domain symbols and is given by $(\mathbf{F} \otimes \mathbf{I}_{N_r})\mathbf{\Theta}^{-1}\mathbf{E}_1\mathbf{\Theta}(\mathbf{F}^{-1} \otimes \mathbf{I}_{N_r})$. Similar to $\mathbf{G}_{\text{RX}}$, the elements of $\tilde{\mathbf{G}}$ are given by $\tilde{g}_q = \frac{1}{N_c} \sum_{n=0}^{N_c-1} j\theta(a, n + N_g) \cdot \exp(-j2\pi qn/N_c)$. Observing (5), the first term is the wanted part of the received MIMO OFDM symbol, whereas the second term signifies the PN contribution which consists of the CPE and the ICI.

To investigate the influence of the different frequency components of the phase noise (PN) spectrum, we consider a sinusoidal PN signal $\theta(a,m) = A\cos(\frac{2\pi\delta}{N_c}(aN_{\text{tot}} + m))$.

Here the peak phase deviation is denoted by A and $\delta = fN_c/f_s$ represents the phase noise frequency (f) normalized to the subcarrier spacing (f_s/N_c), where f_s signifies the sample frequency. The PN process can later on be built up as a summation of these sinusoidal PN signals with different frequencies δ. Applying the sinusoidal PN process and using the first order approximation in (5), $\tilde{g}_q(\delta)$ is given by

$$\tilde{g}_q(\delta) = \frac{A}{2N_c}\left[\frac{\Psi \exp\left(-j\pi(q+\delta)\right)\sin\left(\pi(q+\delta)\right)}{\exp\left(-j\frac{\pi(q+\delta)}{N_c}\right)\sin\left(\frac{\pi(q+\delta)}{N_c}\right)} + \frac{\Psi^* \exp\left(j\pi(q-\delta)\right)\sin(\pi(q-\delta))}{\exp\left(j\frac{\pi(q-\delta)}{N_c}\right)\sin\left(\frac{\pi(q-\delta)}{N_c}\right)}\right] \quad , \quad (6)$$

where $\Psi = \exp(j\frac{2\pi\delta}{N_c}(aN_{tot} + N_g))$. The normalized version is given by $\hat{g}_q = \tilde{g}_q/A$. The normalized PN power weighting function is now found by calculating the power of $\hat{g}_q$, which turns out to be given by (7) (see next page), where $\Re$ denotes the real part. It is noted that the transfer of power by PN in a frequency selective environment and applying a non-constant-amplitude modulation also depends on the channel $\hat{\mathbf{H}}$ and transmitted signal $\hat{\mathbf{s}}(a)$, as seen in (5).

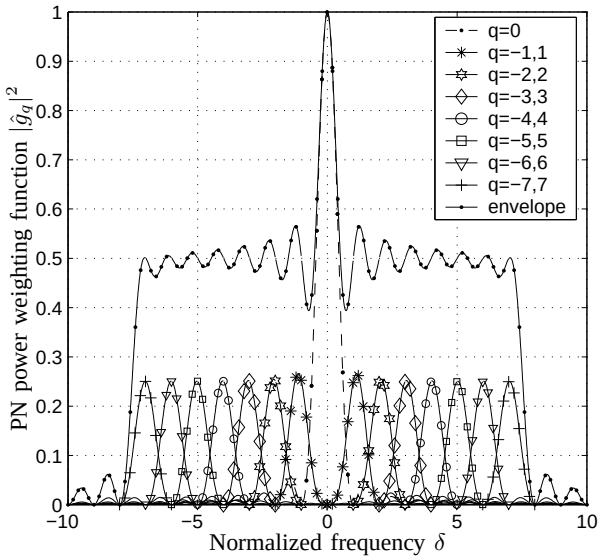

Fig. 2. Normalized PN power weighting function as a function of normalized frequency δ for 15 subcarriers, $N_c = 64$.

In Fig. 2 the normalized weighting function is illustrated for different values of q as function of δ. From the figure the symmetry in both δ and q is obvious. Knowing the weighting function the total PN contribution P_n can be calculated as

$$P_n = \sum_{q=0}^{N_c-1} \int_0^{N_c/2} |\hat{g}_q(\delta)|^2 L_{\text{pn}}(\delta) d\delta \quad , \quad (8)$$

where $L_{\text{pn}}(\delta)$ is the single side band (SSB) noise power spectral density (PSD).

The weighting function is a convenient measure for the spread of the PN power over the different subcarriers and provides insight into the influence of PN in a multicarrier system.

III. Estimation and correction of CPE

In Section II-B we made a distinction between the two phenomena caused by PN after the DFT: a common phase rotation for all carriers (CPE) and an additive ICI term. In this section we propose a method to estimate and correct for this CPE.

When we rewrite (3) to

$$\begin{aligned}\hat{\mathbf{x}} &= \mathbf{G}_{\text{RX}}\hat{\mathbf{H}}\hat{\mathbf{s}} + \hat{\mathbf{n}} \\ &= g_0\hat{\mathbf{H}}\hat{\mathbf{s}} + \mathbf{G}'\hat{\mathbf{H}}\hat{\mathbf{s}} + \hat{\mathbf{n}} \quad , \end{aligned} \quad (9)$$

we see that $g_0 = \frac{1}{N_c}\sum_{n=0}^{N_c-1}\exp\left(j\theta(a, n+N_g)\right)$ is the average rotation of the a-th symbol evoked by the PN. The matrix $\mathbf{G}'$ indicates the influence of the ICI and equals $\mathbf{G}_{\text{RX}} - g_0\mathbf{I}_{N_cN_r}$.

Since the CPE changes on a symbol by symbol basis, an initial correction using the preamble is insufficient to correct for it. Therefore, a convenient way to enable estimation and correction of this CPE on a symbol-by-symbol basis is to insert pilot carriers in the transmitted data symbols. We define $\mathcal{P} = \{p_1, p_2, \ldots, p_P\}$ as the collection of pilot carrier numbers (equal on all TX branches). P is the number of pilot carriers per branch. On the pilot carrier p ($p \in \mathcal{P}$) the $N_r \times 1$ received frequency domain vector $\mathbf{x}(p)$, or observation vector, is given by

$$\mathbf{x}(p) = g_0\mathbf{H}(p)\mathbf{s}(p) + \mathbf{\Lambda}(p) + \mathbf{n}(p) \quad , \quad (10)$$

where the ICI terms are given by $\mathbf{\Lambda} = \mathbf{G}'\hat{\mathbf{H}}\hat{\mathbf{s}}$ and $\mathbf{s}(p)$ for $p \in \mathcal{P}$ are the known pilot symbols. The goal is now to estimate g_0 from the observation vector $\mathbf{x}$ and to correct the received signal $\mathbf{x}$ by multiplying it with g_0^*. The estimate of g_0 is found by optimization of some criterion based on the assumptions of the estimation noise. Here the estimation error, or observation noise, is given by $\mathbf{z}(p) = \mathbf{x}(p) - g_0\mathbf{H}(p)\mathbf{s}(p) = \mathbf{\Lambda}(p) + \mathbf{n}(p)$, which is a summation of ICI and additive white Gaussian noise (AWGN).

A. Maximum Likelihood estimation

Similarly to the derivation in [9], we can, in first instance, not make the assumption that the noise components in the different observations within $\mathbf{x}(p)$ are uncorrelated. This is due to possible correlation in the ICI, since the same LO feeds all RX branches. We assume that the noise $\mathbf{z}(p)$ is multivariate complex normally distributed with the unknown $N_r \times N_r$ covariance $\mathbf{\Omega}$, i.e. $\mathbf{z}(p) \sim \mathcal{CN}(\mathbf{0}, \mathbf{\Omega})$ for $p \in \mathcal{P}$. Furthermore, it is assumed that the estimation error on the different pilot carriers is uncorrelated, but that the noise on the same pilot carriers on the different RX antennas is correlated. Note that this correlation is caused by the ICI term.

The joint probability density function, conditional on all the unknown parameters, is given by [10]

$$p(\mathbf{z}|g_0, \mathbf{\Omega}) = \frac{(\pi)^{-PN_r}}{\det(\mathbf{\Omega})^P}\exp\left(-\sum_{p\in\mathcal{P}}\mathbf{z}^H(p)\mathbf{\Omega}^{-1}\mathbf{z}(p)\right) \quad . \quad (11)$$

$$|\hat{g}_q(\delta)|^2 = \frac{1}{4N_c^2}\left[\frac{\sin^2(\pi(q+\delta))}{\sin^2\left(\frac{\pi(q+\delta)}{N_c}\right)} + \frac{\sin^2(\pi(q-\delta))}{\sin^2\left(\frac{\pi(q-\delta)}{N_c}\right)} + \frac{2\sin(\pi(q+\delta))\sin(\pi(q-\delta))}{\sin\left(\frac{\pi(q+\delta)}{N_c}\right)\sin\left(\frac{\pi(q-\delta)}{N_c}\right)}\Re\left\{\Psi^2\exp\left(j2\pi q\frac{N_c-1}{N_c}\right)\right\}\right] \quad , \quad (7)$$

When we now define the $P \times N_r$ matrix $\mathbf{Z} = [\mathbf{z}(p_1), \mathbf{z}(p_2), \ldots, \mathbf{z}(p_P)]^H$, the joint probability density function of (11) can be written as

$$p(\mathbf{Z}|g_0, \mathbf{\Omega}) = \frac{(\pi)^{-PN_r}}{\det(\mathbf{\Omega})^P}\exp\left(-\mathrm{tr}(\mathbf{Z}\mathbf{\Omega}^{-1}\mathbf{Z}^H)\right) \quad . \quad (12)$$

The maximum likelihood (ML) estimation is then given by maximizing the log-likelihood function $\ln\left(p(\mathbf{Z}|g_0, \mathbf{\Omega})\right)$, which is given by

$$L(g_0, \mathbf{\Omega}) = C_1 + P\ln(\det(\mathbf{\Omega}^{-1})) - \mathrm{tr}\left(\mathbf{Z}\mathbf{\Omega}^{-1}\mathbf{Z}^H\right) \quad , \quad (13)$$

where C_1 denotes a constant. Setting the partial derivative of the log-likelihood function with respect to $\mathbf{\Omega}$ to zero gives the conditional estimate $\bar{\mathbf{\Omega}} = (\mathbf{Z}^H\mathbf{Z})/P$ [11]. When this is substituted in (13), the conditional log-likelihood function is given by

$$L(g_0, \bar{\mathbf{\Omega}}(p_1), ..., \bar{\mathbf{\Omega}}(p_P)) = C_2 - P\ln(\det(\mathbf{Z}^H\mathbf{Z})) \quad , \quad (14)$$

where C_2 denotes a constant. Maximizing this log-likelihood function is then equal to minimizing

$$\mathbf{\Phi}(g_0) = \det(\mathbf{Z}^H(g_0)\mathbf{Z}(g_0)) = \det(\sum_{p\in\mathcal{P}}\mathbf{z}(p)\mathbf{z}^H(p)) \quad . \quad (15)$$

The minimum can be found by setting the partial derivative of the determinant criterion in (15) with respect to g_0 to zero. Other ways to work out this minimization problem are well-established Newton-type iterative techniques [9]. Note that the problem is tedious to solve and that the order of the problem increases with the number of antennas and pilots.

B. Reduced-complexity estimator

To derive a practical estimation technique for system implementation, we simplify the underlying model by diverging from the constraints. We assume that all estimation errors in $\mathbf{z}(p)$ are independent, i.e. the covariance matrix $\mathbf{\Omega}$ in (11) reduces to a diagonal matrix. The determinant of $\mathbf{\Omega}$ then reduces to the product of its elements. Maximizing the log-likelihood function now equals maximizing the exponent term in (12). This is achieved by minimizing

$$\begin{aligned}\mathbf{\Phi}(g_0) &= \mathrm{tr}\left(\mathbf{Z}\mathbf{\Omega}^{-1}\mathbf{Z}^H\right) = \frac{\mathrm{tr}\left(\mathbf{Z}\mathbf{Z}^H\right)}{\sigma^2} \\ &= \frac{1}{\sigma^2}\sum_{p\in\mathcal{P}}\mathbf{z}^H(p)\mathbf{z}(p) = \frac{\mathbf{z}_\mathcal{P}^H\mathbf{z}_\mathcal{P}}{\sigma^2} \\ &= \frac{1}{\sigma^2}\|\mathbf{x}_\mathcal{P} - \bar{g_0}\mathbf{H}_\mathcal{P}\mathbf{s}_\mathcal{P}\|^2 \quad , \end{aligned} \quad (16)$$

where we assumed the estimation noise term to be also white over space, thus $\mathbf{\Omega} = \sigma^2\mathbf{I}_{N_r}$, where σ^2 is the variance of the observation noise. The error vector on the collection of pilot carriers $\mathbf{z}_\mathcal{P}$ is defined as $\mathbf{z}_\mathcal{P} = \mathbf{x}_\mathcal{P} - g_0\mathbf{H}_\mathcal{P}\mathbf{s}_\mathcal{P} = \mathbf{\Lambda}_\mathcal{P} + \mathbf{n}_\mathcal{P}$. Here $\mathbf{z}_\mathcal{P}$ is given by the $PN_r \times 1$ vector $(\mathbf{z}^T(p_1), \mathbf{z}^T(p_2), \ldots, \mathbf{z}^T(p_P))^T$, which is a concatenation of the error vectors $\mathbf{z}$ at the different pilot carriers. The vectors $\mathbf{x}_\mathcal{P}$, $\mathbf{s}_\mathcal{P}$ and $\mathbf{n}_\mathcal{P}$ are similarly built up as a concatenation. The p-th block diagonal element of the $PN_r \times PN_t$ block diagonal channel matrix $\mathbf{H}_\mathcal{P}$ is given by the $N_r \times N_t$ matrix $\mathbf{H}(p)$.

Note that (16) equals the least squares (LS) criterion and that under the assumption of independent white Gaussian noise ML estimation reduces to LS estimation. The well known solution of the LS problem is given by

$$\bar{g_0} = \mathbf{A}_\mathcal{P}^\dagger\mathbf{x}_\mathcal{P} = \left\{\mathbf{A}_\mathcal{P}^H\mathbf{A}_\mathcal{P}\right\}^{-1}\mathbf{A}_\mathcal{P}^H\mathbf{x}_\mathcal{P} \quad , \quad (17)$$

where $\mathbf{A}_\mathcal{P} = \mathbf{H}_\mathcal{P}\mathbf{s}_\mathcal{P}$. Recalling that the channel is quasi-static and if the pilot tones in the packet are equal for the consecutive OFDM symbols, it is sufficient to calculate the pseudo-inverse $\mathbf{A}_\mathcal{P}^\dagger$ only once per packet. Clearly, the complexity of this algorithm is much lower than the minimization of the cost function in (15) for every symbol, which is required for the ML estimation.

It is noted that the 1×1 version of this reduced-complexity algorithm is equal to the one proposed in [5].

C. Accuracy reduced-complexity estimator

Next to complexity, the accuracy of the estimator is of importance. The error in the estimate of (17) is given by $\bar{g_0} - g_0 = \mathbf{A}_\mathcal{P}^\dagger\mathbf{z}_\mathcal{P}$. This shows that the estimator is unbiased, since we defined $\mathbf{z}$ to be zero mean. The covariance of the estimate is given by

$$\begin{aligned}\mathrm{cov}(\bar{g_0}) &= E\left[(\bar{g_0} - g_0)(\bar{g_0} - g_0)^H\right] \\ &= E\left[\left\{\mathbf{A}_\mathcal{P}^H\mathbf{A}_\mathcal{P}\right\}^{-1}\mathbf{A}_\mathcal{P}^H\mathbf{z}\mathbf{z}^H\mathbf{A}_\mathcal{P}\left\{\mathbf{A}_\mathcal{P}^H\mathbf{A}_\mathcal{P}\right\}^{-1}\right] \\ &= \left\{\mathbf{A}_\mathcal{P}^H\mathbf{A}_\mathcal{P}\right\}^{-1}\mathbf{A}_\mathcal{P}^H E\left[\mathbf{z}_\mathcal{P}\mathbf{z}_\mathcal{P}^H\right]\mathbf{A}_\mathcal{P}\left\{\mathbf{A}_\mathcal{P}^H\mathbf{A}_\mathcal{P}\right\}^{-1} \\ &= \sigma^2\left\{\mathbf{A}_\mathcal{P}^H\mathbf{A}_\mathcal{P}\right\}^{-1} \quad , \end{aligned} \quad (18)$$

where σ^2 denotes the variance of the observation noise, which is given by $\sigma_\Lambda^2 + \sigma_n^2$. Here σ_n^2 is the variance of the AWGN and σ_Λ^2 is the covariance of ICI. In the case of perfect orthogonal AWGN channels the covariance is given by

$$\mathrm{cov}(\bar{g_0}) = \frac{\sigma^2}{N_rP} = \frac{\sigma_\Lambda^2 + \sigma_n^2}{N_rP} \quad , \quad (19)$$

where we assumed the total transmit power P_t to be 1. Since g_0 is also frequency dependent, we regard the normalized covariance Υ as a measure of the accuracy of the estimation. Υ is given by

$$\Upsilon = \frac{\mathrm{cov}(\bar{g_0})}{|g_0|^2} = \frac{\sigma_\Lambda^2 + \sigma_n^2}{N_rP|g_0|^2} \quad . \quad (20)$$

Note that Υ equals the mean squared error (MSE). The MSE is frequency dependent, since g_0 and σ_Λ are functions of the frequency.

To derive this frequency dependency of Υ, we consider, similarly to Section II-B, a sinusoidal PN signal $\theta(a,m) = A\cos(\frac{2\pi\delta}{N_c}(aN_{\text{tot}}+m)+\varphi)$. Again the peak phase deviation is denoted by A, $\delta = fN_c/f_s$ represents the phase noise frequency normalized to the subcarrier spacing and φ denotes a uniform distributed random phase. Using this notation, the CPE term is given by

$$g_0 = \tfrac{1}{N_c}\sum_{n=0}^{N_c-1}\exp(jA\cos(\tfrac{2\pi\delta n}{N_c}+\varphi)) \quad . \tag{21}$$

The ICI term is upperbounded by the case in which the elements of $\hat{\mathbf{H}}\hat{\mathbf{s}}$ add constructively to form the ICI. This is achieved when $\hat{\mathbf{H}}\hat{\mathbf{s}}$ equals the $N_cN_r \times 1$ vector $[1,1,\ldots,1]^T$. The ICI for the k-th subcarrier is then given by

$$\Lambda(k) = \frac{1}{N_c}\sum_{\substack{q\neq 0\\ q=-N_c+k}}^{k-1}\sum_{n=0}^{N_c-1}\exp(jA\cos(\frac{2\pi\delta n}{N_c}+\varphi)) \cdot\exp\left(-j2\pi qn/N_c\right) \quad . \tag{22}$$

Here we included $\frac{2\pi\delta}{N_c}(aN_{\text{tot}}+N_g)$ in the random phase φ. Let $b = \frac{2\pi\delta}{N_c}$ and using the derivation in Appendix I, an upper bound on the variance of the ICI term $\sigma_\Lambda^2 = E\{|\Lambda|^2\}$ is given by

$$\hat{\sigma}_\Lambda^2 = \left(\frac{A}{N_c}\right)^2\left\{\frac{\sin^2(\frac{1}{2}N_cb)}{2\sin^2(\frac{1}{2}b)}+\frac{1}{2}N_c^2 -\frac{N_c\sin(\frac{1}{2}N_cb)}{\sin(\frac{1}{2}b)}\cos\left(\frac{1}{2}(N_c-1)b\right)\right\} \quad . \tag{23}$$

Similar as in the derivation of the upper bound on σ_Λ^2 in Appendix I, we find an expression for the power of g_0, independent of φ, by averaging over the random phase φ:

$$|g_0|^2 = 1+\frac{A^2\sin^2(\frac{1}{2}N_cb)}{2N_c^2\sin^2(\frac{1}{2}b)} \quad . \tag{24}$$

Now substituting (23) and (24) in (20) provides a final expression for the MSE Υ of the estimation. Figure 3 depicts the MSE as function of the normalized frequency for different MIMO configurations. The number of carriers and pilots equals 64 and 4, respectively. In this example average SNRs per RX branch of 10, 20 and 30 dB are applied. It is clear from Fig. 3 and (20) that the MSE at low frequencies decreases with N_r, the SNR (and P, although not shown in Fig. 3) and at high frequencies only with N_r. At low frequencies the AWGN dominates the performance, while at higher frequencies the ICI is dominant. The floor at low frequencies is thus determined by the number of RX antennas, pilots and the SNR, while the floor at high frequencies is determined by the number of RX antennas and pilots carriers.

The *low-pass* frequency characteristic of the MSE of the estimation is explained by the fact that the CPE is observed only once every N_{tot} samples. This means that only changes with lower frequencies can be accurately tracked by this estimation algorithm.

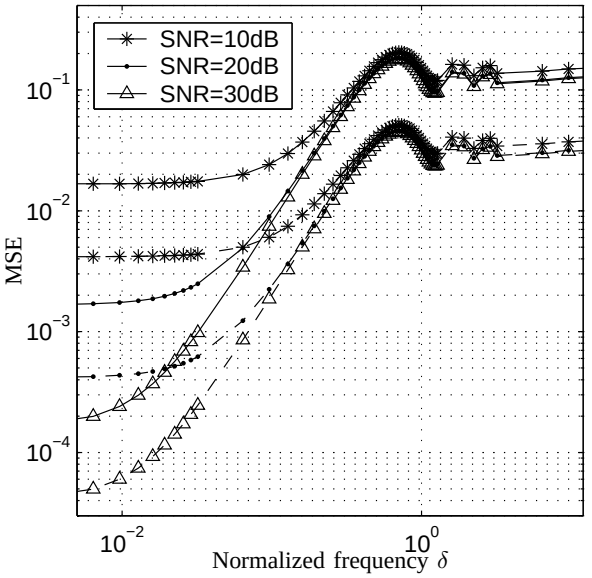

Fig. 3. Theoretical MSE as function of the normalized frequency δ for 1×1 (solid) and 4×4 (dashed) configurations, applying $N_c = 64$, $P = 4$ and SNR of 10, 20 and 30 dB.

IV. Impact of phase noise

A. Modelling of PN

In Section II-B we assumed the PN θ to be a random variable, but made no assumptions about its distribution. For further evaluation we now model the PN as zero-mean white Gaussian noise, with a variance of 1, which is filtered by the PN power spectral density (PSD). The PN PSD of an oscillator is generally modelled using a Lorentzian function with uniform phase distribution. This equals the squared magnitude of a first order low pass filter function. This model is given by (25) and the single side band (SSB) version is depicted in Fig. 4.

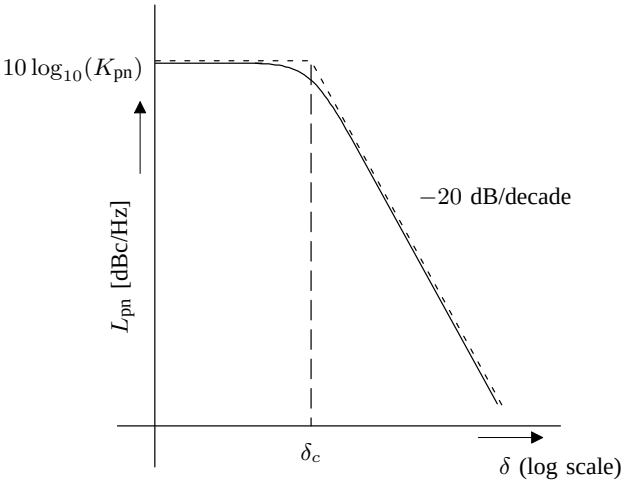

Fig. 4. PSD of the Lorentzian PN model.

The model has two parameters, which are the DC-gain K_{pn} and the corner frequency δ_c. The corner frequency is determined by the bandwidth of the phase lock loop (PLL), which is used in the frequency synthesizer (FS). After the breakpoint δ_c, the PSD falls off with 20 dB per decade. The transfer function of the PSD is given by

$$L_{\text{pn}} = K_{\text{pn}} \frac{1}{1 + (\delta/\delta_c)^2} \quad . \quad 0 \leq |\delta| < N_c/2 \qquad (25)$$

Note that the PSD is given in rad^2/Hz. The total PN power is found by integrating the SSB PN PSD over the spectrum and doubling it to get the double side band (DSB) PN power. The DSB PN power is given by

$$P_{\text{pn}} = \frac{2f_s}{N_c} \cdot \int_0^{N_c/2} \frac{K_{\text{pn}}}{1 + (\delta/\delta_c)^2} d\delta = \frac{K_{\text{pn}} \delta_c \pi f_s}{N_c} \quad , \qquad (26)$$

where we assumed that $\delta_c \gg 0$ and that $\delta_c \ll N_c/2$. The total power in dBc (dB below the carrier power) is given by $10 \log_{10}(P_{\text{pn}})$.

B. Phase Noise after CPE suppression

When we use the suppression of the CPE as proposed in Section III-B, the PN spectrum will be influenced by that. Figure 5 shows an example of the influence of the suppression on the PN PSD. The solid line depicts the original PN PSD as function of frequency, for a Lorentzian PN PSD with a normalized corner frequency $\delta_c = 3.2 \cdot 10^{-2}$ and a total integrated PN power of $P_{\text{pn}} = -30$ dBc. The dashed line shows the compensation as function of the frequency for an infinite SNR. The *dash-dot* line depicts the PN after compensation for the CPE with $\bar{g_0}^*$.

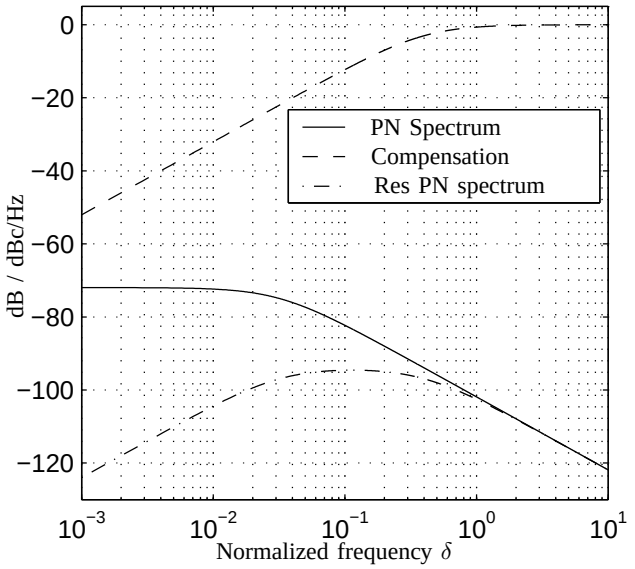

Fig. 5. Example of the influence of the compensation approach for a Lorentzian PN spectrum with $\delta_c = 3.2 \cdot 10^{-2}$ and $P_{\text{pn}} = -30$ dBc.

This figure shows that the compensation is directly related to the MSE of the estimated CPE. Phase errors with low frequencies can be estimated better and thus better compensated. This results in a PN PSD after compensation of which the lower frequency components are suppressed the most. The resulting PN spectrum can easily be found by combining the expression for the MSE of the estimated CPE (20) and the PSD of the PN (25).

V. Simulations results

Simulations were carried out to evaluate the performance of the estimator and to see the performance of a MIMO OFDM system experiencing PN. As a test case a MIMO extension of the 802.11a WLAN standard was studied. The main parameters for the simulation are therefore based on the IEEE 802.11a standard and summarized in Table I.

TABLE I
Simulation parameters, based on the 802.11a OFDM standard

System Parameter	Parameter Value
Modulation	64 QAM
Bandwidth	20 MHz
Number of subcarriers N_c	64
OFDM Symbol duration	4 μs
Guard Interval	800 ns

Figure 6 depicts results of simulations using the reduced-complexity estimator proposed in Section III-B applying a perfect orthogonal AWGN channel. The MSE is depicted as function of the frequency of the sinusoidal PN signal, as defined in Section III-C. The curves are depicted for SNRs of 10 and 30 dB and for a 2×2 and 4×4 MIMO configuration. Furthermore, the figure shows the corresponding curves of the upper bound on the MSE derived in Section III-C.

It is clear from Fig. 6 that the analytical upper bound on MSE is close and follows the simulation results. Though, a tighter upper bound remains a subject for further investigation. Again the relation of the performance and the number of antennas and SNR is as concluded in Section III-C.

It was found from simulations, though not shown here, that the MSE was higher than expected at high frequencies when only a low number of TX antennas was used. This can be explained by high correlation between the received signals when an AWGN channel is used, making also the ICI highly correlated. This correlation invalidates the assumption in Section III-B, that the estimation errors are independent on the different RX branches. That the increase occurs at higher frequencies is explained by the dominance of the ICI on the performance there. It is anticipated that this effect will not occur in faded channels.

Figure 7 depicts the bit-error-rate (BER) and packet-error-rate (PER) performance of a 1×1 and 2×2 MIMO system. A perfect orthogonal AWGN channel was used for simulations and the BER and PER performance are obtained by averaging over 10,000 144 byte packets. The PN PSD of Section IV-A was used in simulations, where the total integrated PN power was P_{pn} was -30 dBc and the corner frequency f_c was varied.

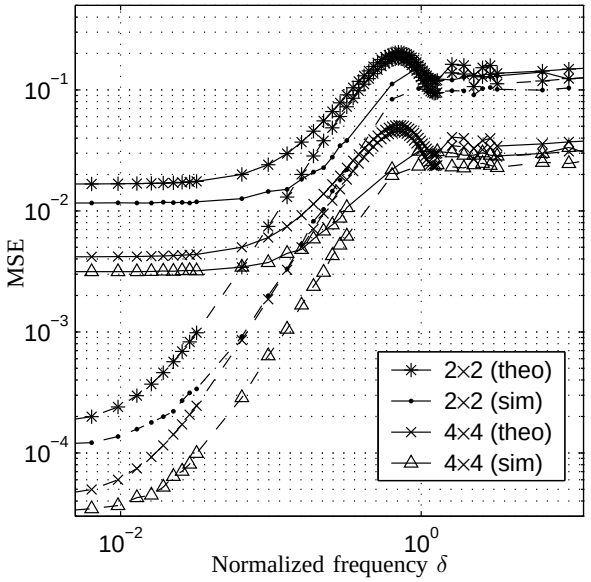

Fig. 6. Theoretical and experimental MSE as function of the normalized frequency for AWGN channel. Top four curves (solid) for SNR = 10 dB, lower four (dashed) for SNR = 30 dB . Every antenna applies 4 pilot carriers, modulation is 64 QAM.

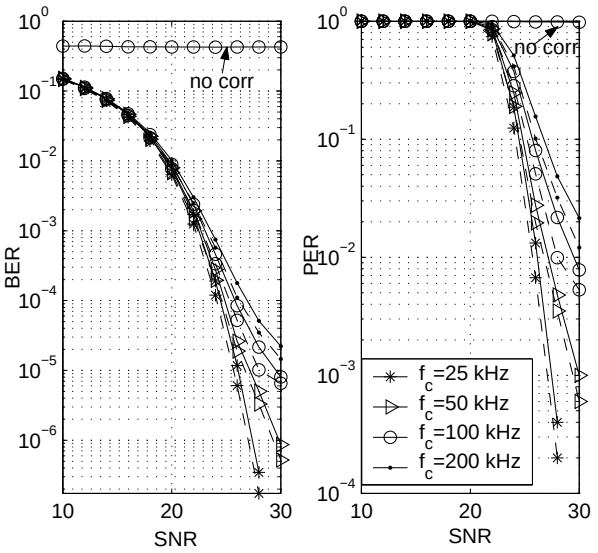

Fig. 7. Raw BER and PER for 1×1 (—) and 2×2 (−−) configuration. AWGN channel and $P_{\text{pn}} = -30$ dBc, packetlength = 144 byte. The curves with *no corr* show the performance without compensation.

The reduced-complexity estimator was used to compensate for the CPE. Vertical BLAST [12] is used as MIMO detection scheme. Furthermore, the figure depicts the performance for the system experiencing the same PN without compensation. Only one curve is depicted for this (1×1, f_c = 100 kHz), since all curves lay on top of each other in the regarded SNR range.

From Fig. 7 it is clear that the 2×2 system performance is better than the one of the 1×1 system, whereas it offers twice the datarate. Additionally, we conclude that the lower the corner frequency f_c the better the performance that is achieved. This can be explained by the fact that the PN suppression of the algorithm is the highest at lower frequencies, as was shown in Fig. 5.

VI. Conclusions and discussion

The influence of phase noise (PN) in a multiple antenna OFDM system was investigated. It was shown that, similarly to conventional OFDM systems, a phase shift common to all carriers and inter-carrier-interference was introduced. Furthermore, a PN power weighting function was derived which can be applied to show the influence of the shape of the PN spectrum.

Additionally, an estimation and compensation approach for the common rotation of the received constellation points, invoked by the PN, was proposed. The maximum likelihood (ML) estimation of PN was shown to be equal to a determinant criterion optimization problem. It was recognized that the complexity of this estimator was too high to be practicable for an implementation, and therefore a reduced-complexity estimator was proposed. An upper bound on the mean-squared-error of this estimator for the AWGN environments was found. A comparison between the performance of the ML estimator and reduced-complexity estimator remains a topic for further study.

Using this bound we found the remaining PN spectrum after compensation. This measure enables designers to take into account this suppression of the PN, when designing a frequency synthesizer. It is clear that the lower frequency components in the PN spectrum are suppressed most by the CPE correction.

As a test case a MIMO extension of the 802.11a WLAN standard was studied. From the simulation results it is clear that the analytical upper bound on the error of the estimator is close. Furthermore, the bit-error-rate (BER) and packet-error-rate (PER) simulations show that the performance is greatly improved by the CPE suppression. Moreover it is clear that PN spectra with a higher corner frequency, so with more power in higher frequencies, show a worse performance than those with a lower corner frequency. These performance simulations again point out that the CPE compensation benefits from the MIMO schemes. Performance in a (correlated) multipath environment remains a topic for further study, but the schemes are anticipated to benefit from the space diversity in that case.

Acknowledgements

This work was carried out within the B4 Broadband Radio@hand project, which is supported in part by the Dutch Ministry of Economic Affairs under grant BTS01063. The authors thank Xiao-Jiao Tao for his useful comments. Furthermore, Allert van Zelst, Peter Smulders and Gert Brussaard are acknowledged for their input to improve the quality of this paper.

APPENDIX I
FREQUENCY DEPENDENCY OF ICI

This appendix shows the derivation of the upper bound on the variance of the ICI due to PN. When we assume all carriers hold data symbols, all carriers on average will experience the same ICI power. We, therefore, regard only one of the carriers, $k = N_c$, and substitute this k into (22). When we define $b = \frac{2\pi\delta}{N_c}$, the ICI term Λ is given by

$$\Lambda = \frac{1}{N_c} \sum_{q=1}^{N_c-1} \sum_{n=0}^{N_c-1} \exp(jA\cos(bn+\varphi)) \exp\left(-j2\pi qn/N_c\right) \quad . \tag{27}$$

Now we can rewrite the Λ as

$$\begin{aligned}
\Lambda &= \frac{1}{N_c} \sum_{q=0}^{N_c-1} \sum_{n=0}^{N_c-1} \left(\exp(jA\cos(bn+\varphi) - j2\pi qn/N_c)\right) - g_0 \\
&= \exp(jA\cos(\varphi)) - g_0 \\
&= \exp(jA\cos\varphi) - \frac{1}{N_c} \sum_{n=0}^{N_c-1} \exp(jA\cos\left(bn+\varphi\right)) \\
&= \frac{\exp(jA\cos\varphi)}{N_c} \sum_{n=0}^{N_c-1} \left(2\sin^2\left\{\frac{A}{2}\left[\cos\left(bn+\varphi\right) - \cos\varphi\right]\right\}\right. \\
&\qquad \left. - j\sin\left\{A\left[\cos\left(bn+\varphi\right) - \cos\varphi\right]\right\}\right) \quad .
\end{aligned} \tag{28}$$

For small values of A, the expression for the ICI in (28) can be approximated as

$$\begin{aligned}
\Lambda &\approx \frac{jA}{N_c} \exp(jA\cos\varphi) \sum_{n=0}^{N_c-1} \left[\cos\left(bn+\varphi\right) - \cos\varphi\right] \\
&= \frac{jA\exp(jA\cos\varphi)}{N_c} \left(\frac{\sin(\frac{1}{2}N_c b)}{\sin(\frac{1}{2}b)} \cos\left(\frac{1}{2}(N_c-1)b+\varphi\right)\right. \\
&\qquad \left. - N_c\cos\varphi\right) \quad .
\end{aligned} \tag{29}$$

Then the amplitude of the ICI is given by $|\Lambda|$

$$|\Lambda| = \frac{A}{N} \left| \frac{\sin(\frac{1}{2}N_c b)}{\sin(\frac{1}{2}b)} \cos\left(\frac{1}{2}(N_c-1)b+\varphi\right) - N_c\cos\varphi \right| \quad , \tag{30}$$

where we used

$$\begin{aligned}
\sum_{n=0}^{N-1} \cos\left(bn+\varphi\right) &= \Re\left\{\sum_{n=0}^{N-1} \exp\left(j\left(bn+\varphi\right)\right)\right\} \\
&= \Re\left\{\exp(j\varphi)\left(\frac{1-\exp\left(jbN\right)}{1-\exp\left(jb\right)}\right)\right\} \\
&= \frac{\sin(\frac{1}{2}N_c b)}{\sin(\frac{1}{2}b)} \cos\left(\frac{(N_c-1)b}{2}+\varphi\right) \quad .
\end{aligned} \tag{31}$$

The solution in (30) is a function of the uniform distributed variable φ. To find the frequency dependency of the normalized covariance in (20), we have to find $\sigma_\Lambda^2 = E\{|\Lambda|^2\}$ independent of φ. Since φ is uniformly distributed between 0 and 2π, the expected value is given by

$$\begin{aligned}
\sigma_\Lambda^2 &= E\{|\Lambda|^2\} = \frac{1}{2\pi}\int_0^{2\pi} |\Lambda\left(\varphi\right)|^2 \,\mathrm{d}\varphi \\
&= \left(\frac{A}{N_c}\right)^2 \left\{\frac{\sin^2(\frac{1}{2}N_c b)}{2\sin^2(\frac{1}{2}b)} + \frac{1}{2}N_c^2\right. \\
&\qquad \left. - \frac{N_c\sin(\frac{1}{2}N_c b)}{\sin(\frac{1}{2}b)} \cos\left(\frac{1}{2}(N_c-1)b\right)\right\} .
\end{aligned} \tag{32}$$

REFERENCES

[1] IEEE 802.11a standard, ISO/IEC 8802-11:1999/Amd 1:2000(E).

[2] IEEE 802.11g standard, Further Higher-Speed Physical Layer Extension in the 2.4 GHz Band.

[3] A. van Zelst and T.C.W. Schenk, "Implementation of a MIMO OFDM based Wireless LAN System", *Accepted for publication in IEEE Trans. on Signal Processing*, March 2003, available from http://tte.ele.tue.nl/radio/people/SchenkT/.

[4] T. Pollet, M. van Bladel and M. Moeneclaey, "BER sensitivity of OFDM systems to carrier frequency offset and Wiener phase noise", *IEEE Trans. on Commun.*, Vol. 43, No. 2/3/4, Feb./Mar./Apr. 1995, pp. 191-193.

[5] A.G. Armada and M. Calvo, "Phase noise and subcarrier spacing effects on the performance of an OFDM communication system", *IEEE Communications Letters*, Vol. 2, No. 1, pp. 11-13, Jan. 1998.

[6] P. Robertson and S. Kaiser, "Analysis of the effects of phase-noise in orthogonal frequency division multiplex (OFDM) systems", *ICC'95 Seattle*, Vol. 3, pp. 1652-1657.

[7] K. Nikitopoulos and A. Polydoros, "Compensation schemes for phase noise and residual frequency offset in OFDM systems", *IEEE Global Telecommun. Conf. 2001*, pp. 330-333, 2001.

[8] R.A. Casas, S.L. Biracree, and A.E. Youtz, "Time Domain Phase Noise Correction for OFDM Signals", *IEEE Trans. on Broadcasting*, Vol. 48, No. 3, pp. 230-236, Sept. 2002.

[9] Y. Bard, "Nonlinear Parameter Estimation", Academic Press, New York, 1974.

[10] A. van den Bos "The multivariate complex normal distribution-a generalization", *IEEE Trans. on Information Theory*, Vol. 41, No. 2, pp. 537-539, March 1995.

[11] Xiao-Jiao Tao, Cai-Rong Cao and Zhen-Ya He, "Passive Target Tracking Using Maximum Likelihood Estimation", *IEEE Trans. on Aerospace and Electronic Systems*, Vol. 32, No. 4, pp. 1348-1354, Oct. 1996.

[12] P.W. Wolniansky, G.J. Foschini, G.D. Golden and R.A. Valenzuela, "V-BLAST: an architecture for realizing very high data rates over the rich-scattering wireless channel", *Proc. 1998 URSI International Symposium on Signals, Systems, and Electronics*, pp. 295-300, 1998.